Materials and Design 30 (2009) 3972–3978

Contents lists available at ScienceDirect

Materials and Design

journal homepage: www.elsevier.com/locate/matdes

Effect of welding speed on microstructural and mechanical properties of friction stir welded Inconel 600

K.H. Song *, H. Fujii, K. Nakata

Joining and Welding Research Institute, Osaka University, 11-1, Mihogaoka, Ibaraki, Osaka 567-0047, Japan

ARTICLE INFO

Article history:
Received 25 March 2009
Accepted 23 May 2009
Available online 13 June 2009

Keywords:
D. Welding
A. Non-ferrous metal

ABSTRACT

In order to evaluate the properties of a friction stir welded Ni base alloy, Inconel 600 (single phase type) was selected. Sound friction stir welds without weld defect were obtained at 150 and 200 mm/min in welding speed, however, a groove like defect occurred at 250 mm/min. The electron back scattered diffraction (EBSD) method was used to analyze the grain boundary character distribution. As a result, dynamic recrystallization was observed at all conditions, and the grain refinement was achieved in the stir zone, and it was gradually accelerated from 19 μm in average grain size of the base material to 3.4 μm in the stir zone with increasing the welding speed. It also has an effect on the mechanical properties so that friction stir welded zone showed 20% higher microhardness and 10% higher tensile strength than those of base material.

1. Introduction

The Ni base super-alloy is widely used in various industries, such as the chemical plants, power plants and jet engines, because it has a good resistance against oxidation and corrosion under severe conditions [1–3]. Fusion welding, such as gas tungsten arc welding (GTAW) and laser welding, is usually utilized to construct these plants and to repair these parts in a power generator [4,5]. However, when fusion welds are applied to the Ni base super-alloy, some problems, especially hot cracking and grain boundary segregation, could be occurred [4,5]. Also, these welds have a limitation to the increase in their physical and chemical characters in the weld zone [4,5]. Therefore, to complement a weak point of fusion welds, application of the friction stir welding which can be applied in the solid state is requested.

Friction stir welding has many advantages compared to fusion welds. It is possible to weld in the solid state and has advantages of defect suppression, such as blow holes, cracking and segregation which often occur in fusion welds [6,7]. Furthermore, there is a low distortion and residual stresses compared to fusion welds [6,7]. Also, it has been reported to have good properties, e.g., physical and chemical, in the stir zone because it has the advantage of controlling the grain refinement [8–11]. Therefore, in case of applying the friction stir welding to Ni base super-alloys, it is possible to control these defects, usually produced in fusion welding. However, the application of friction stir welding on materials with a high melting point, such as Ni base alloys, has rarely been reported [12,13]. Because these materials retain their high strength at high temperature, there is a problem of a slow welding speed when the friction stir welding on these materials was applied. Thus, these researches showed a limitation in the grain refinement and mechanical property increase because it was performed at low speed in welding, less than 100 mm/min, which was considered to be relatively large heat input [12,13]. Therefore, this study was carried out to establish the weld parameters with defect free at higher welding speeds and to increase the mechanical properties, based on the grain refinement in the stir zone.

2. Experimental procedures

The material used in the present study was Inconel 600 alloy of a Ni base super-alloy. The chemical composition of this material is shown in Table 1. To perform the friction stir welding, 37.5 mm × 150 mm × 2 mm plates were used. The WC–Co (tungsten carbide–cobalt) tool with a 15 mm diameter shoulder and a 6 mm diameter and 1.8 mm length probe was used. Friction stir welding was performed at a constant tool rotation speed of 400 rpm, a constant force of 2.3×10^3 kg f, and a welding speed of 150–250 mm/min by the friction stir welding machine. The tool was tilted forward at 3° from the vertical to make a good weld surface, and argon shielding gas was utilized to prevent oxidation of the welded surface.

To observe the macrostructures and microstructures of the friction stir (FS) welded Inconel 600 alloy, the specimens were prepared as follows. The FS welded specimens were cut perpendicular to the welding direction, machined to a 2 mm × 20 mm size and polished with abrasive paper. After this work, the specimens were etched

* Corresponding author. Tel./fax: +81 6 6879 8668.
E-mail address: song@jwri.osaka-u.ac.jp (K.H. Song).

0261-3069/$ - see front matter © 2009 Elsevier Ltd. All rights reserved.
doi:10.1016/j.matdes.2009.05.033

Table 1
Details of chemical composition on Inconel 600 alloy.

Element	Ni	Cr	Fe	Si	Mn	C	S
Mass (%)	76.0	15.5	8.0	0.25	0.50	0.08	0.008

with a solution of 97 ml HCl, 2 ml HNO_3 and 1 ml H_2SO_4 in order to observe the macrostructure and microstructure.

Analysis by electron back scattered diffraction (EBSD) was employed as the analysis method of the grain boundary characteristic distribution (GBCD) of the FS welded Inconel 600 alloy. For this work, samples were also polished using a vibromet and analyzed using OIM incorporated with SEM for the stir zone. The Vickers hardness and tensile test were evaluated to identify the mechanical properties of the base material and weld zone. Transverse hardness measurement was carried out on the cross section of FS welds with a load of 9.8 N, and a dwell time of 15 s was used. Two types of tensile test specimens, (a) and (b) in Fig. 1, were used to evaluate the transverse tensile strength of FS welds and the longitudinal tensile strength of the stir zone, respectively. Also, tensile tests were carried out three times at each parameter to make the reliability.

3. Results and discussion

The macrostructures of the FS weld zone versus the change of the weld speed are shown in Fig. 2. The Inconel 600 welded at 150 mm/min welding speed was successfully welded from the surface to the bottom, and a band structure was observed in the center of the stir zone, as shown in Fig. 2a. The specimen made at 200 mm/min welding speed was welded from the surface to 1.8 mm in depth, and a band structure was also observed in the center of the stir zone similar to that at 150 mm/min, as seen in Fig. 2b. However, the specimen made at 250 mm/min welding speed was welded much shallower depth compared to the 150 and 200 mm/min samples, and a groove defect on the advancing side was occurred, as shown in Fig. 2c. This phenomenon can be explained due to insufficient metallic plastic flow caused by the rotating probe. If there is not enough heat input into the weld material, it is difficult to make a plastic flow so that a groove defect can easily occur [7]. In addition, the depth of the weld zone was gradually decreased by the increase of welding speed, which can also be explained by the decreased heat input. In other words, the decrease of heat input led to increase the resistance of metallic plastic deformation, which results in the decrease in the depth of tool inserted into the base material during the FS welding.

An analysis of SEM image and EDX spectrum on the band structure was performed, and the results are shown in Fig. 3, comparing with that of normal stir zone structure. As a result, the W (tungsten) and Co (cobalt) elements that were main element in the WC–Co tool were observed at area 1 (band structure), as seen in Fig. 3b. However, in case of the area 2 (normal stir zone), these elements of the WC–Co tool were not observed. Therefore, it is considered that the band structure was formed by the severe wear reaction between the material and the tool, resulted in the inclusion of tool elements into the stir zone during the FS welding.

The temperature hysteresis of the stir zone according to the increase of welding speed is shown in Fig. 4. The temperature hysteresis was measured at the plate's backside on the center of the weld zone during the FSW. At 150 mm/min, the maximum temperature was 890 °C in the stir zone, as seen in Fig. 4. However, it was gradually decreased by increasing the welding speed, as a result, it showed to 780 °C at 200 mm/min and 670 °C at 250 mm/min. Also, the increase of welding speed led to increase the relative cooling rate. Therefore, it can be explained that the heat input per unit length of the stir zone decreases by the increase of welding speed, resulted in the increase of the cooling rate.

The microstructural analysis based on the welding speed was examined by the EBSD method, and the results are shown in Fig. 5. The lines in this figure indicate the low angle boundary (lower than 15°, blue line), high angle boundary (higher than 15°, black line) and annealing twin boundary (red line). The Inconel 600 alloy used in this study was a heterogeneous distribution ranging between 5 μm and 45 μm in grain size, with an average grain size of 19 μm, as shown in Fig. 5a. In case of 150 mm/min in welding speed, the microstructure consisted of equiaxed grains ranging between 2 μm and 20 μm in size, with an average grain size of 5.6 μm, which is a significantly refined grain distribution than that of the base material, as seen in Fig. 5b. At 200 mm/min in welding speed, the grain size was gradually refined due to increase in welding speed, as a result, the average grain size was refined to 4.4 μm,

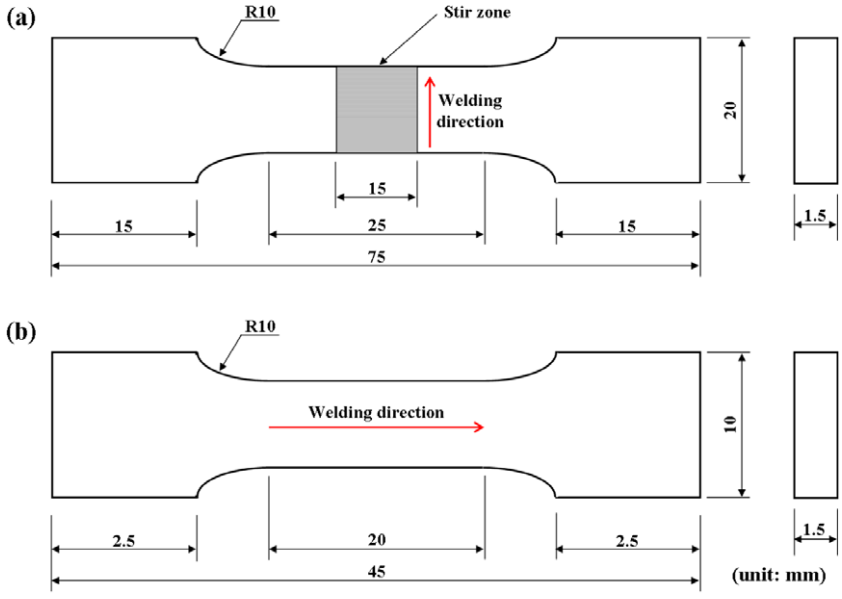

Fig. 1. Configuration of transverse (weld joint) and longitudinal (stir zone) tensile specimens used in the present study. (a) Transverse and (b) longitudinal tensile specimens.

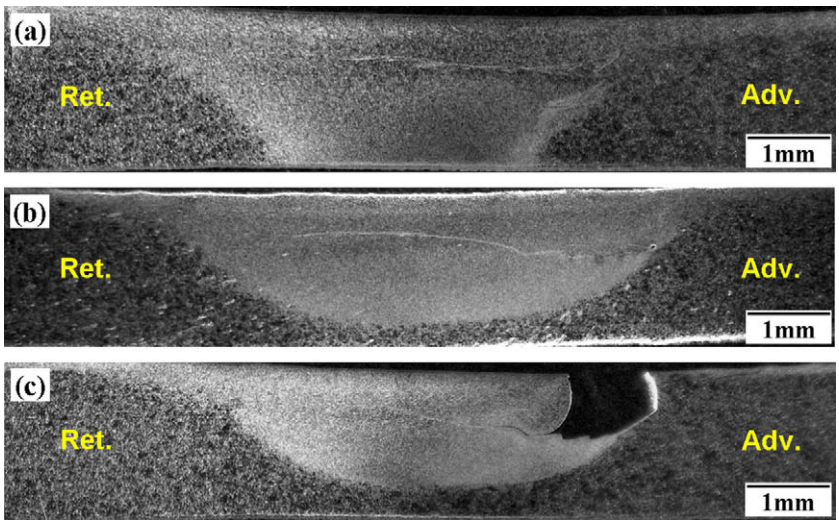

Fig. 2. Macrostructures of weld zone according to weld speed. (a) 150 mm/min, (b) 200 mm/min and (c) 250 mm/min in weld speed.

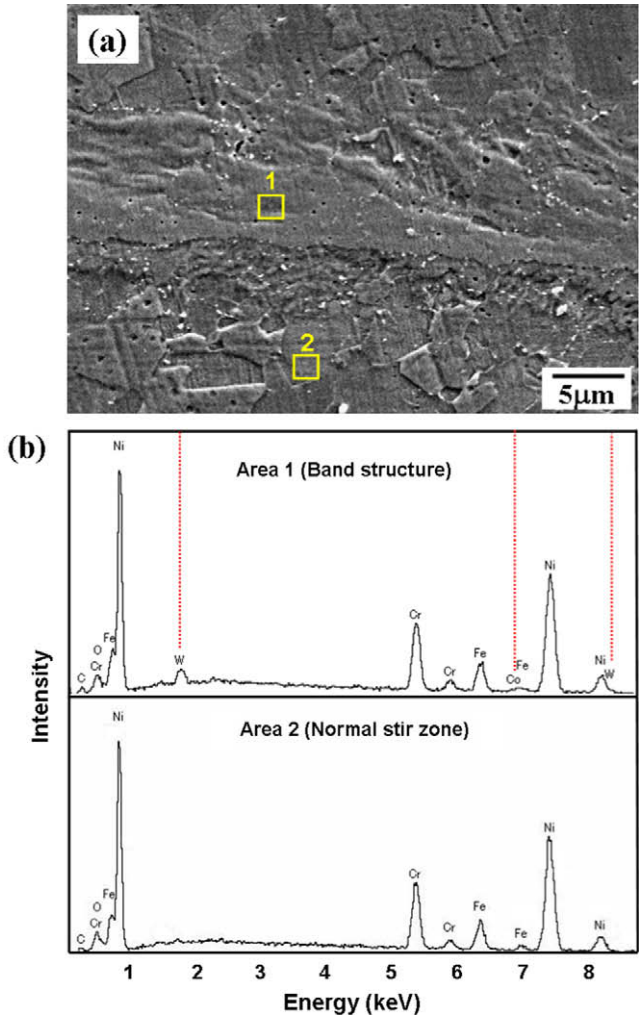

Fig. 3. SEM image and EDS spectrums obtained from the band structure. (a) SEM image and (b) EDS spectrums.

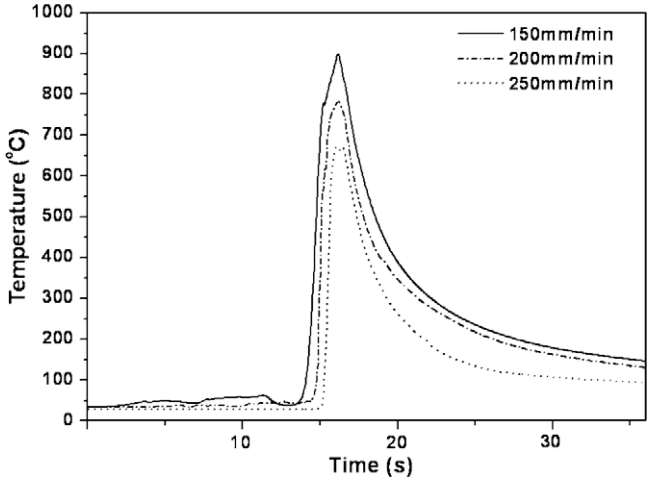

Fig. 4. The temperature hysteresis in the stir zone during the friction stir welding.

as seen in Fig. 5c. The specimen welded at 250 mm/min was a more homogeneous distribution compared to the other conditions, with an average grain size of 3.4 μm, as seen in Fig. 5d. These results clearly show that the increase of welding speed can make a significantly more refined grain distribution than those obtained by Ye et al. (12 μm) and Sato et al. (14 μm) [12,13].

The grain refinement was gradually accelerated by the increase of welding speed, with the constant tool rotation speed. It can be explained in terms of a material with low stacking fault energy such as Ni, Cu, and Pb [14]. These materials are difficult to undergo a rearrangement of their dislocations by dynamic recovery due to the low stacking fault energy, while it is easy to form nuclei for the discontinuous dynamic recrystallization (DDRX), as a result, it can form stable grain nuclei at various sites in the hot deformation microstructure [15]. In other words, it can be explained that grain refinement in this material is accelerated by an increase of the dynamic recrystallization in accordance with the high stored energy, low heat input (but enough to recrystallize due to higher than 550–600 °C (Inconel 600 recrystallization temperature in general)) and high cooling rate.

The misorientation angle distribution according to the increase of welding speed was examined to analyze the aspect of recrystallization, and these results are shown in Fig. 6. At initial state, the base material was distributed by a high angle boundary, more than 96% in fraction, as shown in Fig. 6a. The misorientation angle having 60° was distributed higher than any other degrees, and it was

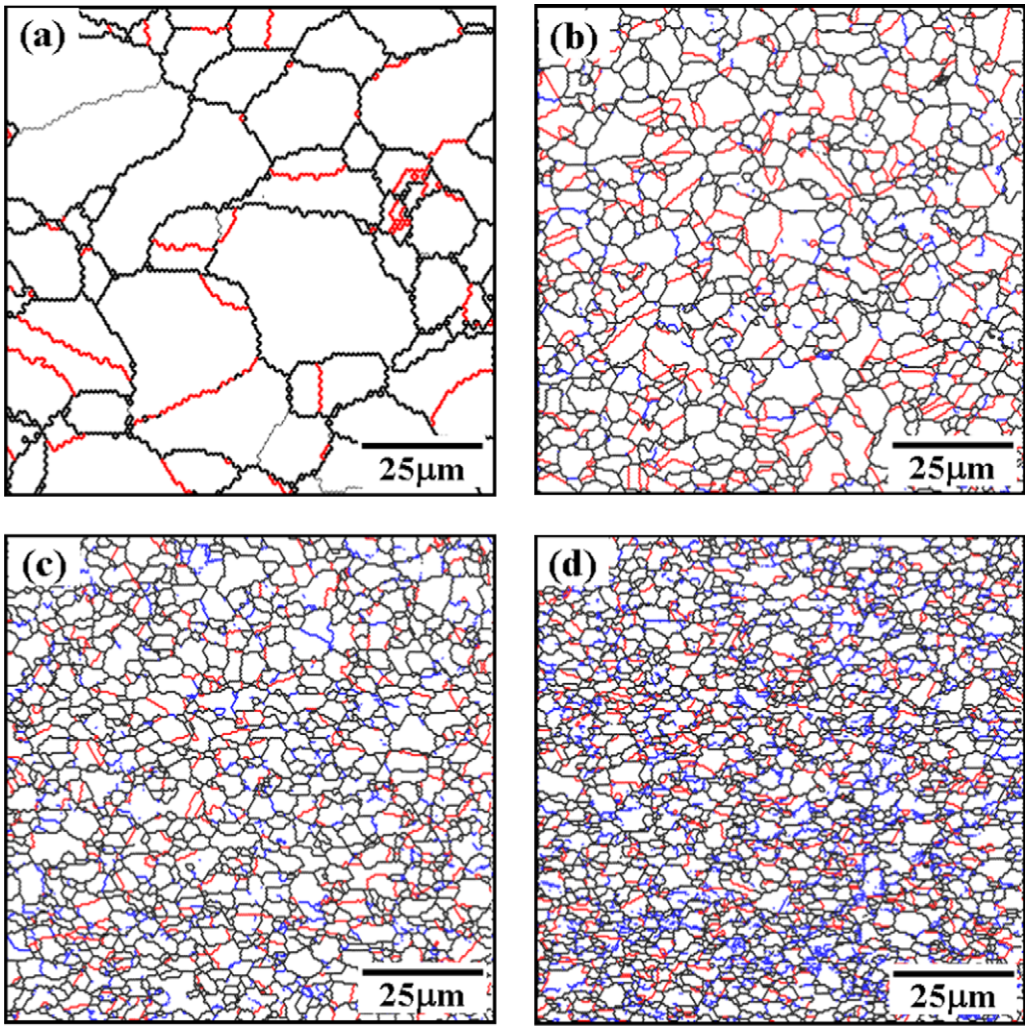

Fig. 5. Grain boundary maps of base material and friction stir welded material. (a) Base material, (b) 150 mm/min, (c) 200 mm/min and (d) 250 mm/min in welding speed; blue, black and red lines show low angle boundary, high angle boundary and annealing twin boundary, respectively. (For interpretation of the references to colour in this figure legend, the reader is referred to the web version of this article.)

identified by the annealing twin boundary, which was usually observed in materials with low stacking fault energy in FCC metals. At 150 mm/min, the high angle grain boundary was distributed over 95%, with 21% annealing twin in fraction, almost the same fraction as the base material, as shown in Fig. 6b. However, by the increasing of welding speed in steps, the low angle boundary distribution was gradually increased, while the high angle boundary distribution was decreased, with 90% at 200 mm/min and 85% at 250 mm/min, as seen in Fig. 6c and d, respectively. In addition, the annealing twin boundary density also was decreased, with 16% at 200 mm/min and 12% at 250 mm/min. Therefore, as the high angle boundary at 150 and 200 mm/min in welding speed was distributed more than 90% in its fraction, it can be considered that dynamic recrystallization was almost achieved in these specimens. However, the increase of the low angle boundary at 250 mm/min can be explained in terms of an insufficient heat input and high cooling rate during the FS welding, which leads to an insufficient dynamic recrystallization. The change of boundary fraction which was observed in Fig. 6 is simply shown in Fig. 7.

The average grain size distributions of the base material and the stir zone are shown in Fig. 8. At the initial state, the base material was distributed with a 19 μm average grain size, as seen in Fig. 8. At 150 mm/min, the average grain size in the stir zone was significantly refined to 5.6 μm compared to the base material, and the increase of the welding speed accelerated the grain refinement, with 4.4 μm at 200 mm/min and 3.4 μm at 250 mm/min. This acceleration of the grain refinement might be affected by the relatively high speed of cooling due to increasing the welding speed.

The microhardness distribution of the weld materials is shown in Fig. 9. The average microhardness of the base material was 163 Hv in Vickers hardness, and that of the stir zone was notably higher than the base material at all the conditions. At 150 mm/min, the microhardness of the stir zone was distributed in the range from 180 to 193 Hv, indicating a greater hardness than the base material. An increase in the welding speed led to an increase in the microhardness of the stir zone, resulted in 180–220 Hv at 200 mm/min and 180–245 Hv at 250 mm/min. The microhardness of the advancing side at all the conditions was found to be higher than those of the retreating side, because the stored energy of advancing side is slightly higher than the retreating side during the welding [16].

The Hall–Petch relationship between the average grain size and microhardness in the center of the stir zone is shown in Fig. 10. As a result, the microhardness distribution versus the increased welding speed satisfied the Hall–Petch relationship. The following relationship was derived, $Hv = 53 + 325d^{-1/2}$. In addition, it is easy to estimate that the effect of dislocation distribution on the microhardness is very low because the low angle boundary in the grains

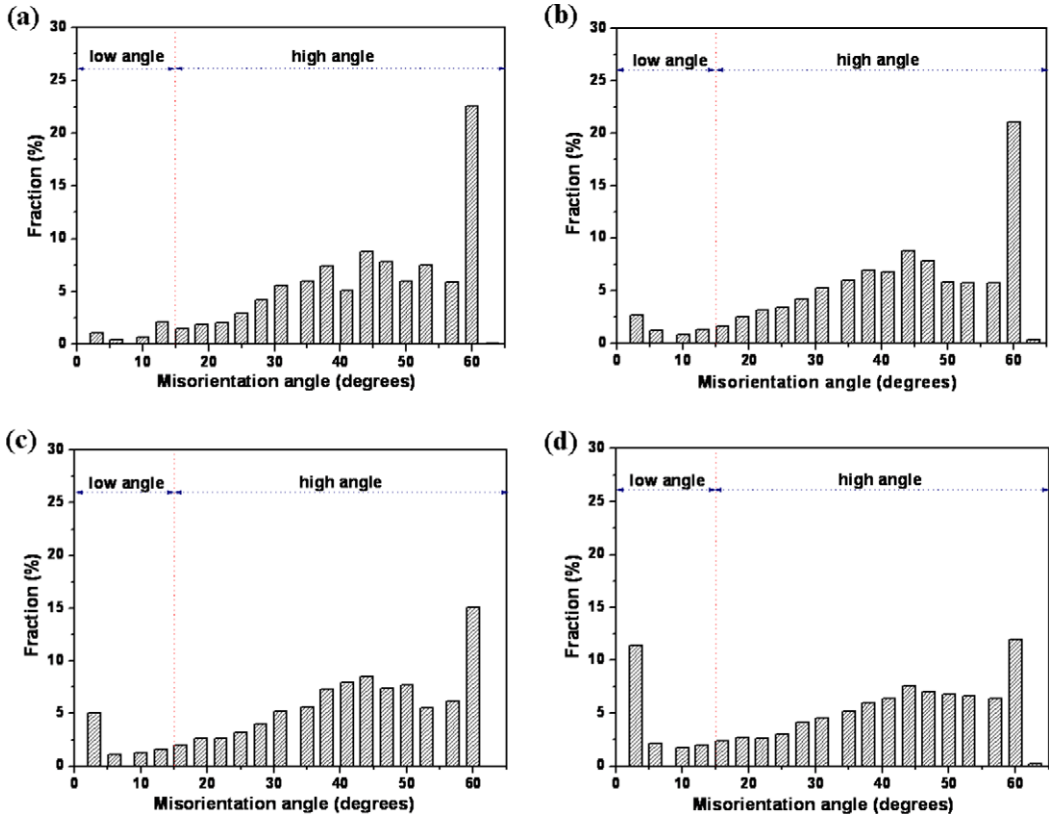

Fig. 6. Changes of grain boundary character distribution by friction stir welding. (a) Base material, (b) 150 mm/min, (c) 200 mm/min and (d) 250 mm/min in weld speed.

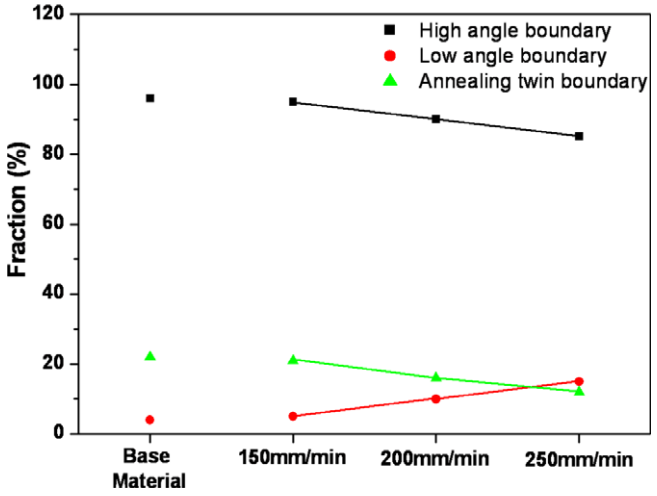

Fig. 7. Changes of misorientation fraction by friction stir welding.

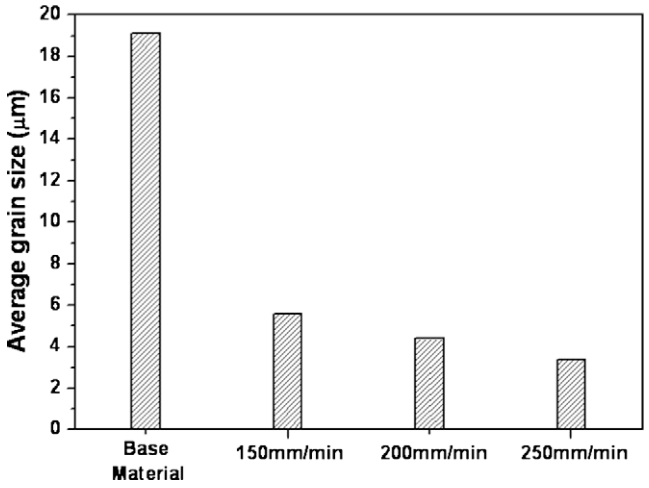

Fig. 8. Changes of average grain size of stir zone according to weld speed.

at all the conditions was not observed, as seen in Fig. 5. Therefore, it can be known that the microhardness gradually increased by the grain refinement.

The appearance of the tensile-tested specimens is shown in Fig. 11. In the base material, it was fractured in the center of the specimen, indicating an elongated shape in the specimen, as seen in Fig. 11a. However, FS welds fractured in the base material at all the conditions, as shown in Fig. 11b and c. This can be considered due to the higher microhardness in the stir zone than that of the base material. Therefore, the base material zone with a relatively low strength was yielded at first and deformed locally, resulted in fracture.

Results of the tensile tests on the FS welded Inconel 600 are shown in Fig. 12. The base material exhibited 683 MPa in ultimate tensile strength (UTS) and 45.6% in elongation, as seen in Fig. 12. For the FS welded specimen on the transverse direction to the FS welding direction, the UTSs were 693 and 699 MPa at 150 and 200 mm/min, respectively, slightly higher than that of the base material, while the elongation were 36.4% and 36.1% at 150 and 200 mm/min, respectively, less than that of the base material due to the localized deformation. On the contrary, in case of the stir zone specimen, the UTS showed 714 and 721 MPa at 150 and 200 mm/min, respectively, obviously higher than that of the base material with comparably large elongations of about 38%, slightly

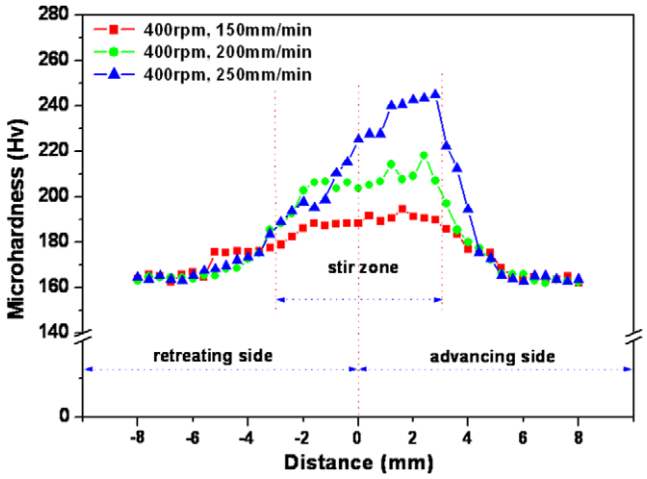

Fig. 9. Distribution of Vickers microhardness in friction stir welded Inconel 600.

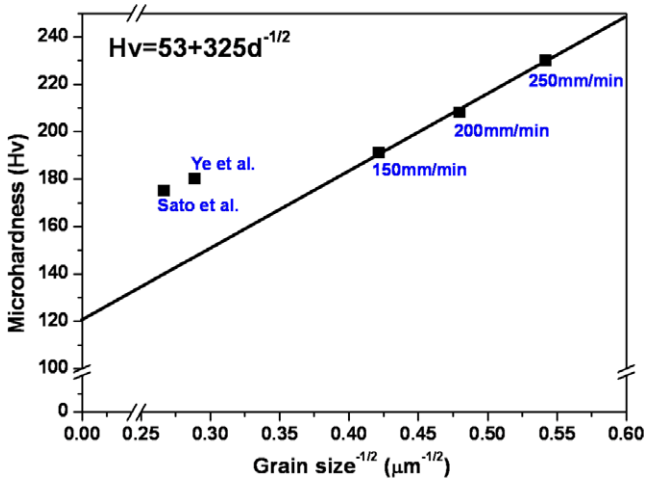

Fig. 10. Hall–Petch relationship between grain size and microhardness according to weld speed in stir zone.

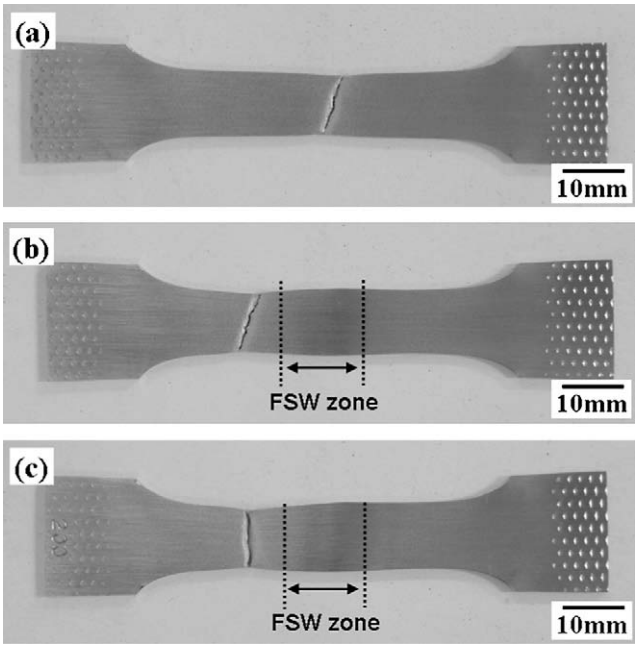

Fig. 11. An external shape of tensile-tested specimens. (a) Base material, (b) 150 mm/min and (c) 200 mm/min in weld speed.

lower than that of the base material. These results apparently showed the reason why the fracture occurred at the base material zone in the transverse tensile specimen of FS welds.

The grain refinement mechanism by FS welding can be simply explained on the basis of plastic flow and dynamic recrystallization. By applying FS welding, the high stored energy in the material was accompanied by severe deformation process. The increase of stored energy by the plastic flow which is the foundation of FS welding can be explained by the increase of dislocation density. Also, an important point for this process is that dynamic recrystallization is accompanied by the friction heat between the tool and material during the FS welding [7]. In addition, as the Inconel 600 alloy used in this study has low stacking fault energy, it is difficult to rearrange the dislocations by dynamic recovery compared to the material with a high stacking fault energy, e.g., Al alloys, while dynamic recrystallization is easy to occur [14,15]. Therefore,

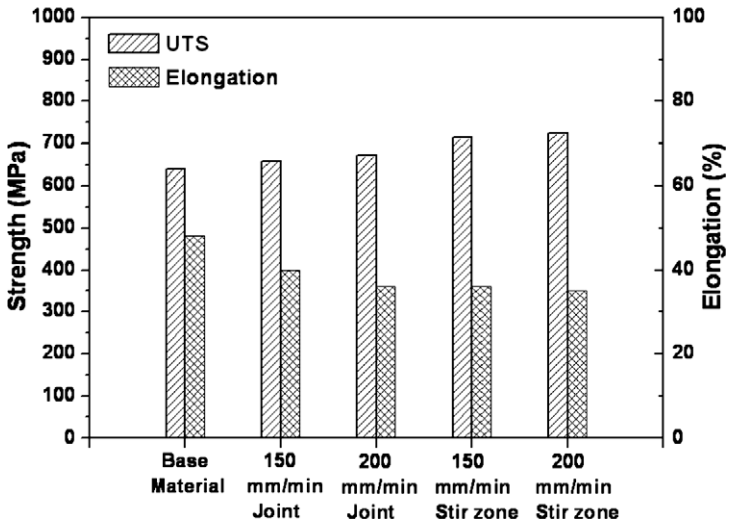

Fig. 12. Transverse (weld joint) and longitudinal (stir zone) tensile properties of friction stir welded Inconel 600 alloy.

when enough heat input and stored energy are provided during the FS welding, formation of the recrystallization nucleus could be occurred coincidentally from the grain boundaries and grains with a high dislocation density. As a result, the microstructure distribution can be obtained with more refined grains than that of the materials, with high stacking fault energy.

4. Conclusions

FS welding of Inconel 600 alloy can be successfully performed at the optimum FS welding conditions at 150 and 200 mm/min of welding speeds and constant tool rotation speed of 400 rpm by using WC–Co tool. Also, the average grain size of the stir zone was markedly refined than that of the base material, which was more accelerated by the increase in welding speed. As a result, the average grain size was gradually refined from 19 μm in the base material to 3.4 μm in the FS welded zone. This grain refinement effectively achieved the increase of mechanical properties. For the microhardness, it was notably increased from 163 Hv in the base material to 245 Hv in the stir zone, and microhardness and grain size relation satisfied the Hall–Petch relationship. The tensile strength also increased from 683 MPa in base material to 721 MPa in the stir zone. Therefore, it is proved that Inconel 600 alloy with low stacking fault energy can effectively achieve the grain refinement, accompanied by the increased mechanical properties, by the FS welding.

Acknowledgement

This work was supported by Grant-in-Aid for Scientific Research (A) from JSPS.

References

[1] Smith WF. Structure and properties of engineering alloys. McGraw-Hill; 1981.
[2] Kim JD, Moon JH. C-ring stress corrosion test for Inconel 600 and Inconel 690 sleeve joint welded by Nd:YAG laser. Corros Sci 2004;46:807–18.
[3] Lim YS, Kim HP, Han JH, Kim JS, Kwon HS. C-ring stress corrosion test for Inconel 600 and Inconel 690 sleeve joint welded by Nd:YAG laser. Corros Sci 2001;43:1321–35.
[4] Kim JD, Kim CJ, Chung CM. Repair welding of etched tubular components of nuclear power plant by Nd:YAG laser. J Mater Process Technol 2001;114:51–6.
[5] Henderson MB, Arrel D, Larsson R, Heobel M, Marchant G. Nickel based superalloy welding practices for industrial gas turbine applications. Sci Technol Weld Join 2004;9:13–21.
[6] Nandan R, Debroy T, Bhadeshia HKDH. Recent advances in friction stir welding – process, weldment structure and properties. Prog Mater Sci 2008;53:980–1023.
[7] Mishra RS, Ma ZY. Friction stir welding and processing. Mater Sci Eng R 2005;50:1–78.
[8] Altenkirch J, Steuwer A, Peel M, Richards DG, Withers PJ. The effect of tensioning and sectioning on residual stresses in aluminium AA7749 friction stir welds. Mater Sci Eng A 2008;488:16–24.
[9] Simar A, Bréchet Y, De Meester B, Denquin A, Pardoen T. Microstructure, local and global mechanical properties of friction stir welds in aluminium alloy 6005A-T6. Mater Sci Eng A 2008;486:85–95.
[10] Balasubramanian V. Relationship between base metal properties and friction stir welding process parameters. Mater Sci Eng A 2008;480:397–403.
[11] Dobriyal RP, Dhindaw BK, Muthukumaran S, Mukherjee SK. Microstructure and properties of friction stir butt-welded AE42 magnesium alloy. Mater Sci Eng A 2008;477:243–9.
[12] Ye F, Fujii H, Tsumura T, Nakata K. Friction stir welding of Inconel alloy 600. J Mater Sci 2006;41:5376–9.
[13] Sato YS, Arkom P, Kokawa H, Nelson TW, Steel RJ. Effect of microstructure on properties of friction stir welded Inconel Alloy 600. Mater Sci Eng A 2008;477:250–8.
[14] Howe JM. Interfaces in materials. Wiley-Interscience; 1997.
[15] Humphreys FJ, Hatherly M. Recrystallization and related annealing phenomena. 2nd ed. Elsevier; 2004.
[16] Sato YS, Nelson TW, Sterling CJ, Steel RJ, Pettersson CO. Microstructure and mechanical properties of friction stir welded SAF 2507 super duplex stainless steel. Mater Sci Eng A 2005;397:376–84.